

## FABRICATION AND CHARACTERIZATION OF LASER MICROMACHINED HOLLOW MICRONEEDLES

S.P. Davis<sup>1</sup>, M.R. Prausnitz<sup>1</sup>, and M.G. Allen<sup>2</sup>  
 School of Chemical Engineering<sup>1</sup> and Electrical and Computer Engineering<sup>2</sup>  
 Georgia Institute of Technology, Atlanta, GA, 30332, USA

### ABSTRACT

Three-dimensional arrays of hollow and solid microneedles have been fabricated using laser micromachining techniques. Excimer (UV) and infrared (IR) laser machining was used to create molds for electrodeposition of metals. Mold materials included polyimide (Kapton), polyethylene terephthalate (Mylar), and titanium. IR laser machining was also used to cut solid needle designs directly from stainless steel. The mechanical stability and insertion characteristics of hollow microneedles were tested. The force necessary for insertion was found to vary linearly with the interfacial area of the microneedle. The force necessary for the fracture of a microneedle was found to increase with tip diameter, wall angle, and wall thickness. Over the range of microneedle geometries tested, the margin of safety between the force for insertion and the force for fracture was the greatest for microneedles with the smallest diameter and the greatest wall thickness.

### INTRODUCTION

We have previously reported the ability of solid silicon microneedles to increase the permeability of *in vitro* skin to a variety of molecules up to three orders of magnitude [1] and that their application to human subjects was painless [2]. In addition, we have reported the benefit of hollow structures increasing the delivery capabilities of microneedles and our ability to create such structures [3]. While these structures have been demonstrated effective in permeabilizing *in vitro* human epidermis, the length limitations (<350  $\mu\text{m}$ ) and tubular shape imposed by previous fabrication techniques have hindered insertion into *in vivo* skin. The viscoelastic nature of living skin requires needles of sufficient length and sharpness to overcome skin's natural deflection to provide reproducible insertion.

Recent work by others in the field [4-6] has revealed a general trend towards hollow, three-dimensional arrays consistent with our initial work. However, the fabrication of these devices often involves relatively complex silicon-based processes. The processing and material expense of these silicon devices may be inappropriate for some high-volume, commodity applications of microneedles.

Laser micromachining has been adopted not only to allow increased needle length and improved insertion characteristics, but also to simplify fabrication and employ the use of metal as a structural material. The use of either

excimer or infrared lasers allows the drilling or cutting of a wide array of materials. Modification of drilling or cutting patterns requires changes only to the CAD program driving the laser and does not require the time necessary to generate new photomasks, as is the case for photolithography-based processing. High-power lasers can also be used to machine arrays through stencil masks in a semi-batch process, ultimately enabling transition to high-volume, continuous roll manufacturing.

### FABRICATION TECHNIQUES

#### Plating of Metal Micromolds for 3D Arrays

Hollow metal microneedles were created from metal molds (Fig. 1). An infrared laser (Resonetics Maestro, Nashua, NH) was used to drill tapered holes through a variety of metals. The drilled metal sheets were then used as sacrificial molds for the formation of microneedles. The tapered shape of the hole was determined primarily by the energy distribution of the beam. The IR laser's Gaussian distribution had a greater fluence at its center than at the edges of the beam and therefore drilled holes with significant taper. A typical geometry includes an entrance diameter 120  $\mu\text{m}$ , exit diameter of 30  $\mu\text{m}$ , and length of 250  $\mu\text{m}$ .

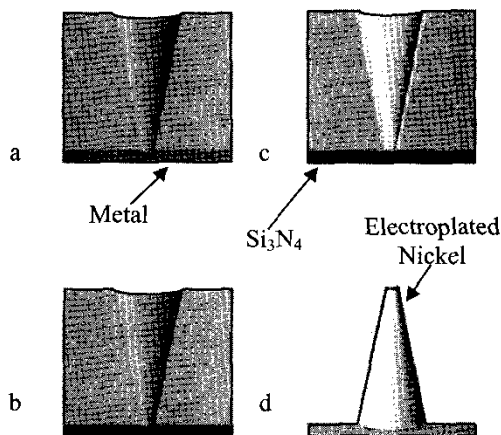


**Figure 1** - Fabrication sequence for microneedles from a metal mold: (a) tapered holes were drilled through metal substrate; (b) Si<sub>3</sub>N<sub>4</sub> was deposited on backside of mold; (c) microneedles were electroplated directly onto mold; (d) the mold was selectively wet etched to free the microneedles.

Initially, the mold material (Ti) was drilled with the desired geometry of holes in an arrangement defined by the drilling program (Fig. 1a). Any redeposition of drilled material on the surface of the mold was removed with mechanical polishing. The backside of the mold was then passivated to prevent electroplating by a 1  $\mu\text{m}$   $\text{Si}_3\text{N}_4$  layer deposited by PECVD (Fig. 1b). The mold was then electroplated with the desired constituent material (Ni) to form the microneedle (Fig. 1c). The base and wall thicknesses of the needles were controlled by adjusting the duration and current density of the electroplating. Finally, the mold was wet etched (HF) to reveal the finished array of microneedles (Fig. 1d and Fig. 2).

The needles generated from this process had the desired tapered, hollow shape. However, the quality of mold generated by IR drilling was not completely satisfactory. Not only was the redeposition of drilled material a concern, but also the sidewalls of the mold were rough, due to the melt and flow process occurring in the laser plasma and the natural isotropy of the metal. In addition, the total height of the needles was still limited by the focal length of the laser itself. This resulted in a height restriction of approximately 250  $\mu\text{m}$ .

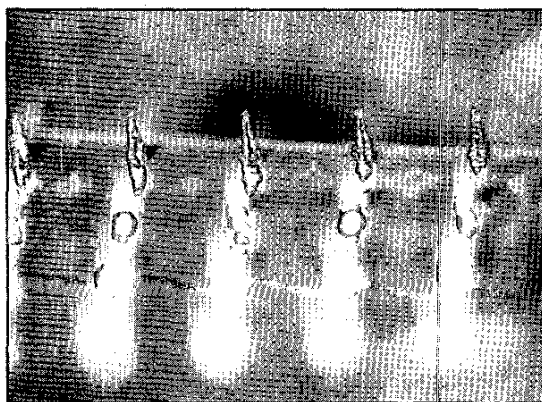


**Figure 2** – Photograph of hollow microneedles created from metal molds. The needles taper from a tip diameter of 50  $\mu\text{m}$  to a base diameter of 180  $\mu\text{m}$  over their 250  $\mu\text{m}$  length. The wall thickness in this case is 10  $\mu\text{m}$ .

### Plating of Polymer Micromolds for 3D Arrays

Hollow metal microneedles were also created from polymer molds (Fig. 3). The processing was similar to the creation of microneedles from metal molds, with the addition of a sputtered seed layer to allow electroplating into a non-conductive mold. A wide variety of polymers are conducive to UV laser drilling and therefore other processing constraints may be taken into consideration in choosing mold materials. In the case of microneedle molding, low cost materials with clean drilling characteristics were desired. Dupont's Mylar and Kapton films both yielded high quality molds, but the low cost and relatively easy removal of Mylar offers a distinct advantage for high volume manufacturing.

Polymer molds were drilled with an excimer laser at 248 nm (Resonetics Micromaster). As in the case of the IR laser, the geometry of drilled features was defined by the energy distribution in the beam. In the case of the KrF laser used in this application, the distribution was a top hat profile. Therefore, a lesser degree of taper was achieved than when using the IR laser. However, since the UV-based removal of polymers was an electronic process as opposed to the melting process of the IR laser, samples had much cleaner sidewalls and little redeposition of drilled material.

In order to achieve the desired taper of drilled holes, the process of simple pulsed laser operation was modified. To form a conical needle, it was desirable to have a circular beam with a region of high energy, or high fluence, at its center with a region of lower energy at its rim. Since changing the distribution of the energy in the beam was not readily achievable, the distribution of energy was modified at the substrate. This was achieved by altering the drilling program to allow trepanning, or tracing, of a circular path whose diameter was less than the diameter of the circular beam. The difference between the beam diameter and the trepanned diameter created a region of beam overlap in the center of the pattern. This overlap resulted in higher fluence at the center of the pattern than the edge, and a correspondingly tapered hole. The diameter of the beam and the trepanned pattern were calculated from the desired hole geometry. A typical geometry is a 250  $\mu\text{m}$  diameter entrance hole and a 50  $\mu\text{m}$  exit through a 500  $\mu\text{m}$  sheet.

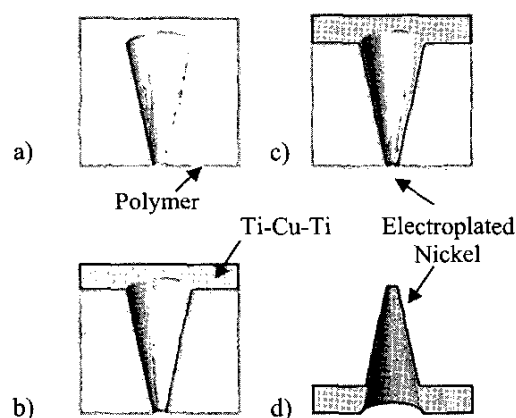


**Figure 3** – Fabrication sequence for microneedles from a polymer mold: (a) tapered holes were drilled through a polymer substrate; (b) a conductive seed layer was deposited on the top and sidewalls of mold; (c) microneedles were electroplated onto the seed layer; (d) the mold was selectively wet etched to free the microneedles.

Once the mold is drilled (Fig 3a), a conformal seed layer is sputter-deposited (Fig 3b). This seed layer is then electroplated to form the microneedles' walls and base (Fig 3c). Finally, the mold is removed with either wet or dry etching depending on the mold material (Fig 3d and 4).

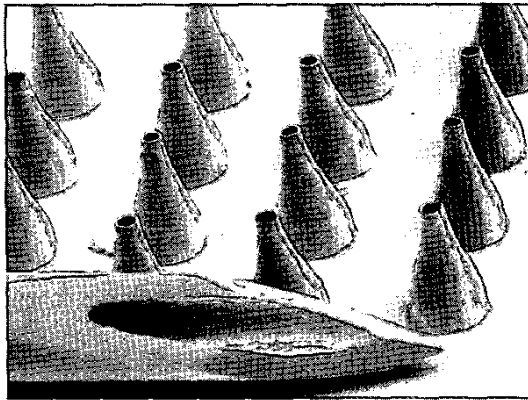


**Figure 4** - Electronmicrograph of hollow microneedles created from polymer molds. The needles taper from a tip diameter of 75  $\mu\text{m}$  to 300  $\mu\text{m}$  at the base over their 500  $\mu\text{m}$  length. The wall thickness in this case is 10  $\mu\text{m}$ . A conventional 27 gauge needle is shown for comparison.

#### Solid Metal 2D and 3D arrays

Solid microneedles were created using IR laser machining (Fig 5). The process was essentially direct-writing in that the beam traced the desired shape of the needle. This results in needles created in the plane of the substrate. The needles may be used as free standing, 2D structures at this point, or may be subsequently bent out of the pane to form a 3D array (Fig. 5). Similar devices created using conventional photolithography on titanium have demonstrated the ability to successfully administer dry-coated antigens to animal models for vaccination [7].

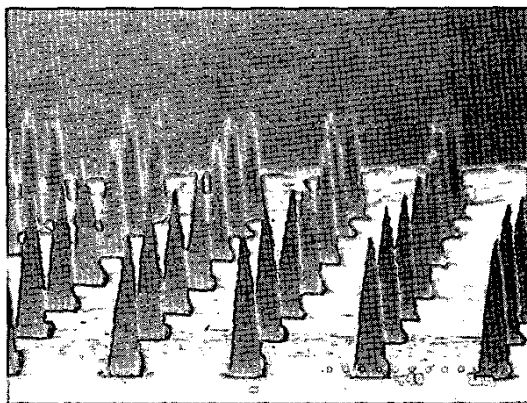


**Figure 5** - Electronmicrograph of solid microneedles cut from stainless steel stock. The needles are approximately 1 mm long and taper from a 250  $\mu\text{m}$  base to a sharp point.

This process offered very rapid production, and as it was not dependant on electroplating, the range of needle materials was expanded. Type 304 stainless steel was selected for its excellent mechanical properties and its pre-existing use as a biocompatible material. As observed

previously, the redeposition of drilled material was a problem when producing high quality microneedles by IR laser micromachining. Thus, redeposited material was electropolished from the stainless steel microneedles to leave clean, high quality samples.

#### MECHANICAL TESTING

The success of microneedles depends on their ability to be reliably inserted into living human skin. Not only must the needles be robust enough to overcome the toughness of skin, but they must also posses the proper geometry to compensate for skin's viscoelastic properties. An understanding of the relationship between these characteristics and needle geometry will allow intelligent design of future generations of needles. The testing of microneedles strength and insertion force was conducted using hollow microneedles generated from polymer molds.

The mechanical strength of microneedles was measured as a function of microneedle geometry using compressive failure testing (EnduraTEC's ScopeTest1, Minnetonka, MN). Fracture force was found to increase with tip diameter, wall thickness, and wall angle (data not shown). Comparison of these experimental results with both finite element simulation and thin shell analytical solution were in good agreement.

The insertion of microneedles of various geometries was studied on human subjects. The force necessary to insert a microneedle was measured by a Tricor Systems 921A Displacement-Force Test Station (Elgin, IL). Since visual determination of insertion is precluded by the deflection of skin, changes in skin's electrical resistance was used to determine the point of insertion (Fig. 6). The relationship between the force necessary for insertion and the interfacial area of the needle tip was found to be linear, which is consistent with a balance between the energy applied to the skin and the energy necessary to create a tear in the skin (data not shown).

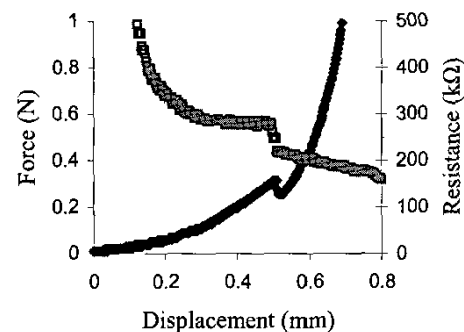


**Figure 6**—The force (●) and electrical resistance (□) experienced by a microneedle during its displacement and insertion into a human subject. The discontinuities in each data set indicate insertion.

Fig. 7 shows both the force necessary to insert microneedles and the force necessary to break microneedles as a function of needle geometry. The plotted values are those generated by the thin shell analytical solution for failure (upper plane) and the upper 95% confidence level of the experimental data collected (lower plane). The margin of safety between these planes varied with microneedle geometry. As the separation between the planes increases so does the margin of safety between the force necessary for insertion and the force to cause microneedle failure. Larger wall thickness and smaller tip diameter offered the greatest margin of safety.

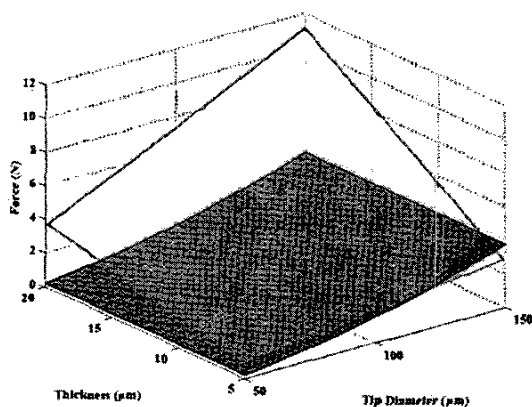


**Figure 7** – Comparison of insertion force and microneedle fracture force. The upper plane is the force necessary to cause the mechanical failure of the microneedle and the lower plane is the force necessary to insert the same microneedle into skin.

## CONCLUSIONS

Three-dimensional hollow and solid microneedle arrays were fabricated using laser micromachining. Both infrared and excimer lasers were used to develop metal and polymer molding processes and direct cutting of metal microneedles. The margin of safety between the mechanical failure of hollow microneedles and the insertion of microneedles varies with geometry. Microneedles with small tip diameters and large wall thickness yielded the greatest margin of safety for mechanical insertion.

## ACKNOWLEDGEMENTS

This work was supported in part by the National Institutes of Health and by the American Diabetes Association. Studies involving human subjects were performed with approval from the Georgia Tech Institutional Review Board. We would like to thank Donald Ackley, Benjamin Landis, Zachary Adams, Harvinder S. Gill.

## REFERENCES

- [1] Henry, S., McAllister, D.V., Allen, M.G., and Prausnitz, M.R. "Microfabricated Microneedles: A Novel Approach to Transdermal Drug Delivery," *J. Pharm. Sci.*, **87**, 922-925 (1998).
- [2] Kaushik, S., A. H. Hord, D. D. Denson, D. V. McAllister, S. Smitra, M. G. Allen, and M. R. Prausnitz, "Lack of Pain Associated with Microfabricated Microneedles," *Anesth. Analg.*, **92**, 502 (2001).
- [3] McAllister, D.V., Cros, F., Davis, S.P., Matta, L.M., Prausnitz, M.R. and Allen, M.G. "Three Dimensional Hollow Microneedle and Microtube Arrays", *Proc. 1999 Int. Conf. on Solid-State Sensor and Actuators Transducers*, Sendai, Japan, 1098-1101 (1999).
- [4] Griss, P., Stemme, G. "Novel, Side Opened Out-of-Plane Microneedles for Microfluidic Transdermal Interfacing." *MEMS 2002, IEEE International Conference, 15<sup>th</sup>*. Las Vegas, NV, 467-470 (2002).
- [5] Gardeniers, J.G.E., Berenschot, J.W., de Boer, M.J., Yeshurun, Y., Hefetz, M., van't Oever, R., and van den Berg, A. "Silicon Micromachined Hollow Microneedles for Transdermal Liquid Transfer." *MEMS 2002, IEEE International Conference, 15<sup>th</sup>*. Las Vegas, NV, 141-144 (2002).
- [6] Stoeber, B., Liepmann, D. "Two-Dimensional Arrays of Out-of-Plane Needles." *Proc. ASME MEMS Div., IMECE*, **2**, 355-359 (2000).
- [7] Matriano, J.A., Cormier, M., Johnson, J., Young, W.A., Buttery, M., Nyam, K, and Daddona, P.E. "Macroflux<sup>®</sup> Microprojection Array Patch Technology: A New and Efficient Approach for Intracutaneous Immunization." *Pharmaceutical Research*, **19**(1), 63-70 (2002).